Electrocaloric properties of epitaxial strontium titanate films

J. Zhang, I. B. Misirlioglu, S. P. Alpay, and G. A. Rossetti

Citation: Appl. Phys. Lett. **100**, 222909 (2012); doi: 10.1063/1.4721668
View online: http://dx.doi.org/10.1063/1.4721668
View Table of Contents: http://apl.aip.org/resource/1/APPLAB/v100/i22
Published by the American Institute of Physics.

Electrocaloric properties of epitaxial strontium titanate films

J. Zhang,[1] I. B. Misirlioglu,[2] S. P. Alpay,[1,3] and G. A. Rossetti, Jr.[1,a)]
[1]*Materials Science and Engineering Program and Institute of Materials Science, University of Connecticut, Storrs, Connecticut 06269, USA*
[2]*Faculty of Engineering and Natural Sciences, Sabancı University, Tuzla-Orhanlı, 34956 Istanbul, Turkey*
[3]*Department of Physics, University of Connecticut, Storrs, Connecticut 06269, USA*

(Received 7 April 2012; accepted 3 May 2012; published online 1 June 2012)

The electrocaloric (EC) response of strontium titanate thin films is computed as a function of misfit strain, temperature, electric field strength, and electrode configuration using a nonlinear thermodynamic theory. For films in a capacitor configuration on compressive substrates, the transition between paraelectric and strain-induced ferroelectric tetragonal phases produces a large adiabatic temperature change, $\Delta T = 5$ K, at room temperature for electric field changes $\Delta E = 1200$ kV/cm. For films on tensile substrates, the transition between the paraelectric and strain-induced ferroelectric orthorhombic phases can also be accessed using inter-digitated electrodes (IDEs). The maximum EC response occurs for IDEs with a [110] orientation. © *2012 American Institute of Physics*. [http://dx.doi.org/10.1063/1.4721668]

The pyroelectric and electrocaloric (EC) effects in polar dielectric solids result from the coupling between the electrical and thermal properties. In the EC effect, an adiabatic change in temperature (ΔT) is produced in response to a change in the applied electric field (ΔE).[1–3] Recent research shows that several thin film ferroelectric (FE) systems [including Pb(Zr,Ti)O_3 (PZT),[4,5] $PbMg_{1/3}Nb_{2/3}O_3$–$PbTiO_3$ (PMN–PT),[6–8] co-polymers,[9] and $SrBi_2Ta_2O_9$ (Ref. 10)] may yield very large adiabatic temperature changes ($\Delta T > 10$ K), one to two orders of magnitude greater than in monolithic FEs.[11] Thermodynamic models combining the Maxwell relations and the Landau theory of phase transformations,[12–15] molecular dynamics,[16] phase-field approaches,[17] Monte Carlo simulations,[18] and first-principles calculations[19] have all been used to understand the origins of the EC effect in different types of FE materials and to model their EC properties under different choices of electrical, thermal, and mechanical boundary conditions.

One interesting class of materials with EC properties that have so far not been explored is incipient FEs such as $SrTiO_3$ (STO). STO undergoes a ferroelastic phase transition from the prototypical cubic perovskite [$Pm\bar{3}m$] to a tetragonal [$I4/mcm$] structure at 105 K due to the rotations of TiO_6 octahedra about the pseudo-cube axes. Although STO crystals or polycrystalline ceramics remain paraelectric down to 0 K, the FE phase can be induced by uniaxial stress,[20] an external electrical field,[21] or doping.[22] A thermodynamic analysis by Pertsev *et al.*[23,24] has shown that it is possible to induce a variety of different FE phases in epitaxial thin films of STO that are not stable in monolithic single-crystal or polycrystalline forms. Following this work, ferroelectricity at room temperature (RT $\cong$ 300 K) in epitaxial (001) STO thin films was observed experimentally by carefully adjusting the equi-biaxial in-plane misfit strain.[25] One of the important features of the Pertsev phase diagram is that it shows that the misfit strain can be used to access two or three different FE phases depending on the temperature (between $\sim 150\,\text{K} < T < \sim 350\,\text{K}$). By adjusting the sign and magnitude of the misfit strain, it was predicted that FE states with out-of-plane or in-plane spontaneous polarizations (along [001] and [100]/[010] of the STO film, respectively) can be generated.[22,23] Because the derivative of the FE polarization with respect to temperature typically shows a sharp maximum near paraelectric to FE phase transitions, an enhancement in the EC response can be expected. Here we show that the RT adiabatic temperature change ΔT of epitaxial (001) STO films can be controlled by the misfit strain and by varying the thermal and electrical boundary conditions. Depending on the electrode configuration [uniform metal-insulator-metal (MIM) or inter-digitated electrodes (IDE)] and on the field strength, the results demonstrate that a RT ΔT of 1–5 K can be achieved in STO films on *both tensile and compressive substrates*.

We consider here a (001) monodomain epitaxial STO film on a thick (001) cubic substrate. Taking into account the equi-biaxial in-plane misfit strain u_m and an applied electrical field E_i, the free energy density of the film by can be expressed as[23,24]

$$\begin{aligned} G(P_i, q_i, u_m, E_i, T) &= G_0 + \tilde{a}_1(P_1^2 + P_2^2) + \tilde{a}_3 P_3^2 + \tilde{a}_{11}(P_1^4 + P_2^4) + \tilde{a}_{33}P_3^4 \\ &+ \tilde{a}_{12}P_1^2P_2^2 + \tilde{a}_{13}(P_1^2 + P_2^2)P_3^2 + \tilde{b}_1(q_1^2 + q_2^2) + \tilde{b}_3 q_3^2 \\ &+ \tilde{b}_{11}(q_1^4 + q_2^4) + \tilde{b}_{33}q_3^4 + \tilde{b}_{12}q_1^2q_2^2 + \tilde{b}_{13}(q_1^2 + q_2^2)q_3^2 \\ &- \tilde{t}_{11}(P_1^2q_1^2 + P_2^2q_2^2) - \tilde{t}_{33}P_3^2q_3^2 - \tilde{t}_{12}(P_1^2q_2^2 + P_2^2q_1^2) \\ &- \tilde{t}_{13}(P_1^2 + P_2^2)q_3^2 - \tilde{t}_{31}P_3^2(q_1^2 + q_2^2) - t_{44}P_1P_2q_1q_2 \\ &- \tilde{t}_{44}(P_1P_3q_1q_3 + P_2P_3q_2q_3) + (C_{11} + C_{12} \\ &- 2C_{12}^2/C_{11})u_m^2 - E_1P_1 - E_2P_2 - E_3P_3, \end{aligned} \quad (1)$$

where G_0 is the free energy density of the paraelectric cubic phase, P_i are the components of the polarization vector, q_i are the structural order parameters describing the rotation of the TiO_6 octahedra, and C_{ij} are the elastic moduli at constant P_i and q_i in Voigt notation. The re-normalized coefficients $\tilde{a}_i$ and $\tilde{a}_{ij}$, $\tilde{b}_i$ and $\tilde{b}_{ij}$, and $\tilde{t}_{ij}$ entering Eq. (1) are given by[23,24]

a)Author to whom correspondence should be addressed. Electronic mail: rossetti@ims.uconn.edu.

$$\tilde{a}_1 = a_1 - \left(g_{11} + g_{12} - 2\frac{C_{12}}{C_{11}}g_{12}\right)u_m,$$
$$\tilde{a}_3 = a_1 + 2\left(\frac{C_{12}}{C_{11}}g_{11} - g_{12}\right)u_m, \quad (2a)$$

$$\tilde{a}_{11} = a_{11} - \frac{g_{12}^2}{2C_{11}}, \quad \tilde{a}_{33} = a_{11} - \frac{g_{11}^2}{2C_{11}}, \quad (2b)$$

$$\tilde{a}_{12} = a_{12} - \frac{g_{12}^2}{C_{11}}, \quad \tilde{a}_{13} = a_{12} - \frac{g_{11}g_{12}}{C_{11}} - \frac{g_{44}^2}{2C_{44}}, \quad (2c)$$

$$\tilde{b}_1 = b_1 - \left(\lambda_{11} + \lambda_{12} - 2\frac{C_{12}}{C_{11}}\lambda_{12}\right)u_m,$$
$$\tilde{b}_3 = b_1 + 2\left(\frac{C_{12}}{C_{11}}\lambda_{11} - \lambda_{12}\right)u_m, \quad (2d)$$

$$\tilde{b}_{11} = b_{11} - \frac{\lambda_{12}^2}{2C_{11}}, \quad \tilde{b}_{33} = b_{11} - \frac{\lambda_{11}^2}{2C_{11}}, \quad (2e)$$

$$\tilde{b}_{12} = b_{12} - \frac{\lambda_{12}^2}{C_{11}}, \quad \tilde{b}_{13} = b_{12} - \frac{\lambda_{11}\lambda_{12}}{C_{11}} - \frac{\lambda_{44}^2}{2C_{44}}, \quad (2f)$$

$$\tilde{t}_{11} = t_{11} + \frac{g_{12}\lambda_{12}}{C_{11}}, \quad \tilde{t}_{33} = t_{11} + \frac{g_{11}\lambda_{11}}{C_{11}}, \quad (2g)$$

$$\tilde{t}_{12} = t_{12} + \frac{g_{12}\lambda_{12}}{C_{11}}, \quad \tilde{t}_{13} = t_{12} + \frac{g_{12}\lambda_{11}}{C_{11}}, \quad (2h)$$

$$\tilde{t}_{31} = t_{12} + \frac{g_{11}\lambda_{12}}{C_{11}}, \quad \tilde{t}_{44} = t_{44} + \frac{g_{44}\lambda_{44}}{C_{44}}, \quad (2i)$$

where a_i and a_{ij}, b_i and b_{ij}, and t_{ij} are the stress-free, monodomain dielectric stiffness coefficients, structural order parameter susceptibility coefficients, and coupling coefficients between the polarization P_i and the structural order parameter q_i, respectively. In Voigt notation, g_{ij} are the electrostrictive constants and λ_{ij} are the coupling coefficients between the strain and q_i.

Using Eqs. (1) and (2), the equations of state $\partial G/\partial P_i = 0$ and $\partial G/\partial q_i = 0$ at $E_i = 0$ and the values of the property coefficients for STO given in Ref. 23, we obtain the identical misfit u_m–T phase diagram of epitaxial monodomain STO films as given by Pertsev *et al.*[24] Figure 1 shows the stability regions of various phases for $150\,\mathrm{K} < T < 400\,\mathrm{K}$ and $-0.02 < u_m < 0.02$. The possible phases and their corresponding order parameters that appear in Figs. 1(a) and 1(b) are HT: $P_1 = P_2 = P_3 = 0$, $q_1 = q_2 = q_3 = 0$; ST: $P_1 = P_2 = P_3 = 0$, $q_1 = q_2 = 0$, $q_3 \neq 0$; FTI: $P_1 = P_2 = 0$, $P_3 \neq 0$, $q_1 = q_2 = q_3 = 0$; FTII: $P_1 = P_2 = 0$, $P_3 \neq 0$, $q_1 = q_2 = 0$, $q_3 \neq 0$; FOI: $|P_1| = |P_2| \neq 0$, $P_3 = 0$, $q_1 = q_2 = q_3 = 0$. We limit ourselves to these ranges of T and u_m since lower operating temperatures are not of great interest for EC cooling devices and misfit strains larger than 2% in magnitude (depending on the substrate material and film thickness) would be partially or completely relaxed via the formation of two-dimensional periodic arrays of interfacial dislocations.[26] The effect of misfit dislocations can certainly be incorporated into the model using an "effective" substrate lattice parameter,[27] but this would unnecessarily complicate the physical interpretation of the results and would obscure the effect of u_m.

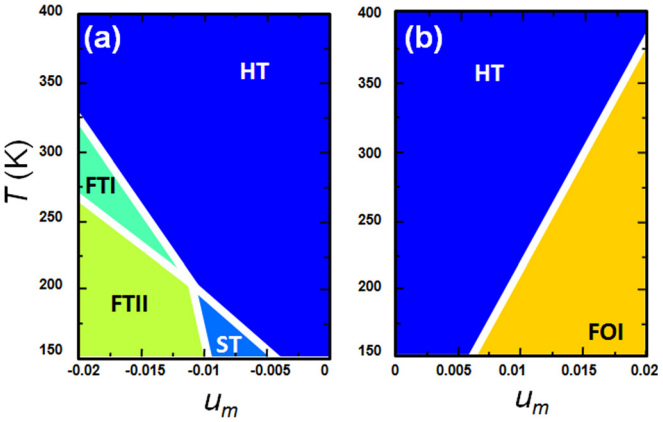

FIG. 1. Misfit strain *vs.* temperature phase diagram of epitaxial monodomain (001) $SrTiO_3$ films. The order parameters of the phases appearing in this map are HT: $P_1 = P_2 = P_3 = 0$, $q_1 = q_2 = q_3 = 0$; ST: $P_1 = P_2 = P_3 = 0$, $q_1 = q_2 = 0$, $q_3 \neq 0$; FTI: $P_1 = P_2 = 0$, $P_3 \neq 0$, $q_1 = q_2 = q_3 = 0$; FTII: $P_1 = P_2 = 0$, $P_3 \neq 0$, $q_1 = q_2 = 0$, $q_3 \neq 0$; FOI: $|P_1| = |P_2| \neq 0$, $P_3 = 0$, $q_1 = q_2 = q_3 = 0$.

Figure 1 shows that depending on u_m and T, three FE phases (FTI, FTII, and FOI) can be stabilized by the lattice mismatch between the film and the substrate. For example, at $T = 225\,\mathrm{K}$ and $-0.0127 < u_m < 0.0106$, the HT phase is stable. The HT phase is a tetragonally distorted but nonpolar variation of the parent cubic ($Pm\bar{3}m$) phase. The tetragonality [i.e., $(c\text{-}a)/a$, where c and a are the lattice parameters of the HT phase] is positive (negative) for $u_m < 0$ ($u_m > 0$) and is zero for $u_m = 0$ for which $c = a = a_0$, where a_0 is the lattice parameter of unconstrained STO. For tensile misfit strains $u_m > 0.0106$, the FE FOI phase (which has an equi-biaxial in-plane spontaneous polarization) stabilizes, while for compressive misfit strains $u_m < -0.0127$, the FE FTI phase is stabilized with an out-of-plane spontaneous polarization along the [001] direction. At this temperature, a transition to the FTII phase occurs for compressive misfit strains $u_m < -0.0144$. This transformation involves the rotation of the TiO_6 octahedra characterized by the structural order parameter q_i and produces a change in the magnitude of polarization along the [001] direction. Hence, the magnitude of the polarization in any of the three FE phases depends on both u_m and T.

The adiabatic temperature change ΔT for the FE phases can be explicitly calculated from the relation[14]

$$\Delta T(T, E_i, u_m) = \sum_{i=1}^{3}\left(-\int_{E_a}^{E_b}\frac{T}{C_E^0(T, E_i, u_m)} \cdot \left(\frac{\partial P_i^0(T, E_i, u_m)}{\partial T}\right)_{E_i} dE_i\right), \quad (3)$$

where the equilibrium polarization $P_i^0(T, E_i, u_m)$ and the equilibrium structural parameter $q_i^0(T, E_i, u_m)$ are obtained from the equations of state for P_i and q_i. The integration limits E_a and E_b define the magnitude of the field change, $\Delta E = E_b - E_a$. Here, the volumetric specific heat $C_E^0(T, E_i, u_m)$ was estimated by adding the computed values of the excess specific heat to the lattice contributions taken from experimental data.[28]

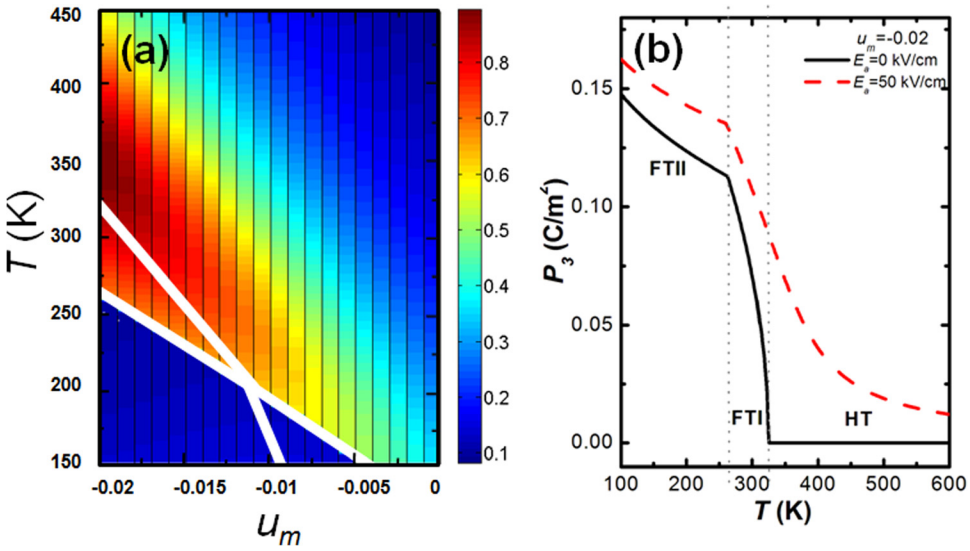

FIG. 2. (a) The adiabatic temperature change ΔT of an epitaxial (001) $SrTiO_3$ film in a MIM configuration as a function of u_m and T for $E_a = 50$ kV/cm and $\Delta E = 120$ kV/cm; (b) the out-of plane polarization P_3 as a function of temperature at $u_m = -0.02$ for $E_a = 0$ kV/cm and $E_a = 50$ kV/cm.

A MIM construct having a (001) epitaxial STO film sandwiched between uniform metallic electrodes is considered first. For this configuration, $E_i = [0, 0, E_3]$ and it is assumed that the bottom electrode is grown pseudomorphically onto the substrate so that both the sign and magnitude of u_m are entirely controlled by the mismatch between the film and the substrate. As can be appreciated from Fig. 1, compressive misfit strains favor the FE phases FTI and FTII while tensile misfit strains favor the FE phase FOI. Because both the HT and ST phases are non-polar and because the component of polarization $P_3 = 0$ is parallel to the field direction E_3, the region of interest is restricted to compressive misfit strains $u_m < -0.01$. This is illustrated in Fig. 2(a), which shows a two-dimensional pseudo-color plot of the adiabatic temperature change ΔT as a function of u_m and T for a particular choice of bias field $E_a = 50$ kV/cm and field change $\Delta E = 120$ kV/cm. As expected for conventional FE materials such as $BaTiO_3$ and $PbTiO_3$,[14] the largest EC response occurs near the paraelectric to FE (HT–FTI) phase transition ($T = 325$ K) where the $P_3(T)$ curve experiences an inflection point and the derivative $\partial P_3/\partial T$ passes through a steep minimum. However, at the comparatively low field level of 120 kV/cm, the maximum adiabatic temperature change is modest, $\Delta T < 1$ K. The reason for this can be understood from Fig. 2(b) where it is seen that the polarization induced along [001] by a field $E_3 = 50$ kV/cm is quite small. It is further apparent that the EC response is not significantly enhanced near the FTI–FTII phase boundary, because at this transition $P_3(T)$ shows only a small change in slope that is accompanied by comparatively small but discontinuous change in $\partial P_3/\partial T$. It is evident from Fig. 2 that to obtain a larger ΔT, the field strength and/or bias field must be increased. Figure 3 shows how ΔT varies as a function of field change ΔE at RT. It is seen in this figure that for field changes $\Delta E = 1200$ kV/cm, a large ΔT of ~5 K can be achieved in STO films at RT. As a point of reference, at these field levels, the EC response for [001] STO in a MIM configuration is closely comparable to that observed in high-quality relaxor PMN-PT films[7] near the temperature of the Curie maximum (~350 K). From this it can be concluded that, as shown for $BaTiO_3$,[14] a relatively small bias field (~50 kV/cm) is sufficient to destroy the discontinuity in polarization at the HT–FTI transition.

Finally, we show that by using an IDE configuration, it is possible to apply in-plane electric fields[29] and by so doing access the HT-FOI phase transformation that occurs under tensile misfit strains. Two IDE configurations are considered; one for which $E_i = [E_1, 0, 0]$ (or $[0, E_2, 0]$) oriented along [100] (or [010]) and a second for which $E_i = [E_1/\sqrt{2}, E_1/\sqrt{2}, 0]$ oriented along [110]. Pseudo-color plots of the adiabatic temperature change as functions of misfit strain and temperature are shown in Figs. 4 and 5 under the same conditions as the MIM configuration shown in Fig. 2 (bias field $E_a = 50$ kV/cm and field change $\Delta E = 120$ kV/cm). As seen in Fig. 4, the largest EC response ($\Delta T = 0.9$ K) for the configuration with $E_i = [E_1, 0, 0]$ occurs near the HT-FOI phase transformation, due to the strong coupling between the in-plane electrical field and the in-plane spontaneous polarization P_1 or (P_2) of the FOI phase. For an IDE configuration with $E_i = [E_1/\sqrt{2}, E_1/\sqrt{2}, 0]$, the largest EC response ($\Delta T = 1.2$ K) is about 30% higher than for the configuration with $E_i = [E_1, 0, 0]$. This can be explained by the fact that for the FOI phase with [100] or [010] IDEs, the electric field only induces polarization along one of the components

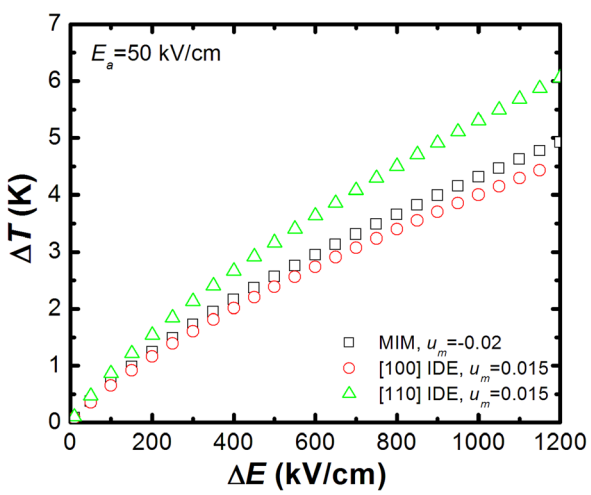

FIG. 3. The room-temperature adiabatic temperature change ΔT of epitaxial (001) $SrTiO_3$ films with MIM ($u_m = -0.020$, open squares) and [100]/[010] and [110] IDE configurations ($u_m = 0.015$, open circles and triangles, respectively) as a function of ΔE for $E_a = 50$ kV/cm.

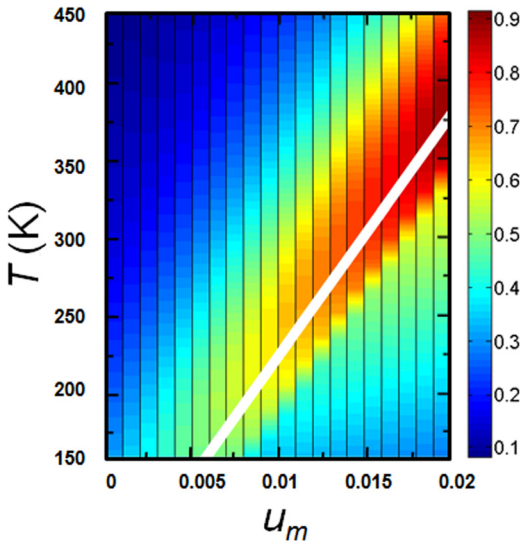

FIG. 4. The adiabatic temperature change ΔT of an epitaxial (001) $SrTiO_3$ film in a [100] IDE configuration as a function of u_m and T for $E_a = 50\,\text{kV/cm}$ and $\Delta E = 120\,\text{kV/cm}$.

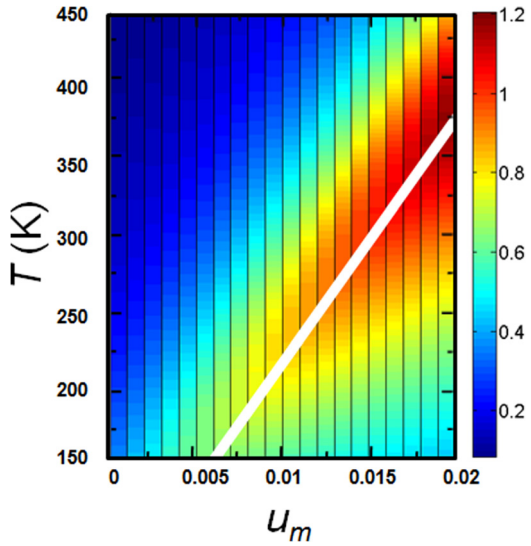

FIG. 5. The adiabatic temperature change ΔT of an epitaxial (001) $SrTiO_3$ film in a [110] IDE configuration as a function of u_m and T for $E_a = 50\,\text{kV/cm}$ and $\Delta E = 120\,\text{kV/cm}$.

(P_1 or P_2), while for [110] IDEs, the applied field induces polarization in both components P_1 and P_2 with a magnitude of $|P| = \sqrt{P_1^2 + P_2^2}$. Comparing the results presented in Figs. 2, 4, and 5 it is seen that, under equivalent electrical boundary conditions, both MIM and IDE configurations have comparable EC responses ($\Delta T \sim 1\,\text{K}$) at RT if the misfit strain is adjusted such that this temperature lies near either the HT–FTI or the HT–FOI phase transformation. The EC response as a function ΔE for the two IDE geometries is compared with that of the MIM configuration in Fig. 3. As seen in the figure, all three configurations can produce a large ΔT ($\sim 5\,\text{K}$) at fields greater than 1000 kV/cm. As expected, the response is slightly larger for the [110] configuration compared with the [100] IDE or MIM.

In summary, we have computed the EC response of STO films as a function of the misfit strain, temperature, applied electric field strength, and electrode configuration. It was shown that for STO films on compressive substrates the EC response can be enhanced in a MIM configuration with uniform electrodes by exploiting the HT–FTI transition. At fields of $\sim$1000 kV/cm the computed temperature change $\Delta T = 5\,\text{K}$ is comparable to FE films near the Curie point. Alternatively, for STO films on tensile substrates the EC response can be enhanced by using an IDE configuration that exploits the HT–FOI transition, with the maximum response occurring for a [110] IDE orientation. Compared with MIM configurations, STO films utilizing an IDE configuration may offer possibilities to increase the EC response while minimizing the dead volume of electrodes. These results show that the strain-induced EC properties of incipient FEs are closely comparable to the measured EC response of conventional or relaxor FEs.

J.Z. would like to thank the Scientific and Technological Research Foundation of Turkey (TÜBITAK) for the Research Fellowship Award for Foreign Citizens that supported her stay at the Sabancı University in Istanbul, Turkey. I.B.M. thanks Turkish Academy of Sciences-GEBİP program for financial support.

[1]J. D. Childress, J. Appl. Phys. **33**, 1793 (1962).
[2]E. Fatuzzo, H. Kiess, and R. Nitsche, J. Appl. Phys. **37**, 510 (1966).
[3]P. D. Thacher, J. Appl. Phys. **39**, 1996 (1968).
[4]R. Chukka, J. W. Cheah, Z. Chen, P. Yang, S. Shannigrahi, J. Wang, and L. Chen, Appl. Phys. Lett. **98**, 242902 (2011).
[5]A. S. Mischenko, Q. Zhang, J. F. Scott, R. W. Whatmore, and N. D. Mathur, Science **311**, 1270 (2006).
[6]Z. Feng, D. Shi, R. Zeng, and S. Dou, Thin Solid Films **519**, 5433 (2011).
[7]A. S. Mischenko, Q. Zhang, R. W. Whatmore, J. F. Scott, and N. D. Mathur, Appl. Phys. Lett. **89**, 242912 (2006).
[8]T. M. Correia, J. S. Young, R. W. Whatmore, J. F. Scott, N. D. Mathur, and Q. Zhang, Appl. Phys. Lett. **95**, 182904 (2009).
[9]S. G. Lu, B. Rozic, Q. M. Zhang, Z. Kutnjak, and B. Neese, Appl. Phys. Lett. **98**, 122906 (2011).
[10]H. Chen, T.-L. Ren, X.-M. Wu, Y. Yang, and L.-T. Liu, Appl. Phys. Lett. **94**, 182902 (2009).
[11]D. Q. Xiao, Y. C. Wang, R. L. Zhang, S. Q. Peng, J. G. Zhu, and B. Yang, Mater. Chem. Phys. **57**, 182 (1998).
[12]G. Akcay, S. P. Alpay, J. V. Mantese, and G. A. Rossetti, Jr., Appl. Phys. Lett. **90**, 252909 (2007).
[13]G. Akcay, S. P. Alpay, G. A. Rossetti, Jr., and J. F. Scott, J. Appl. Phys. **103**, 024104 (2008).
[14]J. Zhang, A. A. Heitmann, S. P. Alpay, and G. A. Rossetti, Jr., J. Mater. Sci. **44**, 5263 (2009).
[15]J. Karthik and L. W. Martin, Appl. Phys. Lett. **99**, 032904 (2011).
[16]Q. Peng and R. E. Cohen, Phys. Rev. B **83**, 220103 (2011).
[17]B. Li, J. B. Wang, X. L. Zhong, F. Wang, and Y. C. Zhou, J. Appl. Phys. **107**, 014109 (2010).
[18]S. Lisenkov and I. Ponomareva, Phys. Rev. B **80**, 140102 (2009).
[19]S. Prosandeev, I. Ponomareva, and L. Bellaiche, Phys. Rev. B **78**, 052103 (2008).
[20]H. Uwe and T. Sakudo, Phys. Rev. B **13**, 271 (1976).
[21]J. Hemberger, M. Nicklas, R. Viana, P. Lunkenheimer, A. Loidl, and R. Bohmer, J. Phys.: Condens. Matter **8**, 4673 (1996).
[22]J. G. Bednorz and K. A. Muller, Phys. Rev. Lett. **52**, 2289 (1984).
[23]N. A. Pertsev, A. K. Tagantsev, and N. Setter, Phys. Rev. B **61**, R825 (2000).
[24]N. A. Pertsev, A. K. Tagantsev, and N. Setter, Phys. Rev. B **65**, 219901 (2002).
[25]J. H. Haeni, P. Irvin, W. Chang, R. Uecker, P. Reiche, Y. L. Li, S. Choudhury, W. Tian, M. E. Hawley, B. Craigo, A. K. Tagantsev, X. Q. Pan, S. K. Streiffer, L. Q. Chen, S. W. Kirchoefer, J. Levy, and D. G. Schlom, Nature (London) **430**, 758 (2004).
[26]I. B. Misirlioglu, S. P. Alpay, M. Aindow, and V. Nagarajan, Appl. Phys. Lett. **88**, 102906 (2006).
[27]J. S. Speck, A. Seifert, W. Pompe, and R. Ramesh, J. Appl. Phys. **76**, 466 (1994).
[28]D. Ligny and P. Richet, Phys. Rev. B **53**, 3013 (1996).
[29]W. K. Simon, E. K. Akdogan, A. Safari, and J. A. Bellotti, Appl. Phys. Lett. **87**, 082906 (2005).